

Preintegrated IMU Features For Efficient Deep Inertial Odometry

R. Khorrambakht, H. Damirchi, and H. D. Taghirad, Senior Member, IEEE

Faculty of Electrical and Computer Engineering

K.N. Toosi University of Technology

P.O. Box 16315-1355, Tehran, Iran

Email: r.khorrambakht, hdamirchi@email.kntu.ac.ir, taghirad@kntu.ac.ir

Abstract—MEMS Inertial Measurement Units (IMUs) are inexpensive and effective sensors that provide proprioceptive motion measurements for many robots and consumer devices. However, their noise characteristics and manufacturing imperfections lead to complex ramifications in classical fusion pipelines. While deep learning models provide the required flexibility to model these complexities from data, they have higher computation and memory requirements, making them impractical choices for low-power and embedded applications. This paper attempts to address the mentioned conflict by proposing a computationally, efficient inertial representation for deep inertial odometry. Replacing the raw IMU data in deep Inertial models, preintegrated features improves the model's efficiency. The effectiveness of this method has been demonstrated for the task of pedestrian inertial odometry, and its efficiency has been shown through its embedded implementation on a microcontroller with restricted resources.

Index Terms—Preintegration theory, deep inertial odometry, convolutional neural networks, embedded AI systems, pedestrian tracking

I. INTRODUCTION

With the advent of MEMS Inertial Measurement Units (IMUs), this proprioceptive sensing modality has seeped into the many gadgets that people carry around every day. Smartphones and smartwatches, automobiles, VR¹ headsets, and even gaming consoles all contain some variant of this sensor. On the other hand, the availability of this sensor for consumer robotics applications has brought them an invaluable source of motion measurement whose measurements are fused with other sensors to assist in accurate localization and state estimation.

The expense for their lower cost though, is that MEMS IMUs are much more challenging to be accurately modeled due to the manufacturing imperfections, high noise, and non-linear effects. While many prominent classical pipelines based on statistical sensor fusion and optimization systems exist for efficient incorporation of such sensors into various applications [1], [2], there are many scenarios where the restricting assumptions made in these classical algorithms gets violated and renders them impractical. Pedestrian inertial odometry, human activity recognition, and robust robotics ego-motion estimation are examples of such applications.

With the emergence of tools for exploiting GPUs in scientific computing and the collection of abundant masses of data,

the deep learning research has reemerged into a revolutionizing field of research in computer science. The particular strength of these models is their ability to learn high-dimensional latent representations from data. Therefore, many researchers in various fields of science have begun to formulate elaborate problems in the context of deep pipelines.

Solving the inertial odometry and motion analysis problems using deep learning has recently gained attention in the literature. Generally, there are two lines of research in this field. Many works try to exploit the deep learning models as modules within a classical fusion system to address their shortcomings. For instance, [3] proposes using an LSTM for detecting zero foot's velocity in human walking, which consequently resets the states of an EKF filter to avoid the accumulation of error. In a similar work, [4] designs a classifier that detects specific motion modes of wheeled vehicles and uses the classifier's results to define a set of pseudo measurements to be used by an Invariant Extended Kalman Filter.

On the other hand, the other group of works casts the problem as a pure data-driven pipeline and synthesizes models that directly consume Raw sensor data to yield the final prediction. For instance, [5] proposes a CNN model for fusing the data from multiple IMUs installed on a human for recognizing his/her activity. In addition, [6] proposes using an LSTM model for predicting the human motion represented in polar coordinate. Furthermore, many works focus on fusing the inertial data with other modalities such as vision [7], [8], and thermal images [9] to estimate the ego-motion of a robot or autonomous vehicle.

While the first approach is computationally efficient, inherited from its classical core, it is highly limited to the design domain for which it was hand-crafted so, the pipeline may not be directly adapted to other applications. On the other hand, even though the second data-driven methods are highly flexible and general, they lack computational efficiency compared to their classical counterparts, and they may not be easily used for embedded and low-power applications.

This paper aims to address this conflict by proposing an efficient and compact motion feature vector which draws inspiration from the preintegration theory known to the graph-based visual-inertial odometry community [10]. This input vector may then be utilized instead of the raw data when the need for efficiency is a top priority. We demonstrate

¹Virtual Reality

the effectiveness of this method for the task of pedestrian inertial odometry using the IO-Net [7] model as a baseline for comparison. Finally, the efficiency of this approach is further illustrated by providing an embedded implementation on a microcontroller with highly restricted resources.

The rest of this paper is organized as follows. Section two introduces the Preintegrated features and describes the network architectures and training procedures for the models. Next, in section three, the experimental results have been presented, and finally, in section four, the concluding remarks and future works have been stated.

II. THE PROPOSED METHOD

A. IMU Model and Preintegration Theory

IMUs measure the instantaneous acceleration and angular velocity expressed in the sensor body frame. Their measurements may be integrated to propagate the object's motion in the inertial frame using the following recursive physics model [10]:

$$\begin{aligned} R_{n+1} &= R_n \text{Exp}((\tilde{\omega}_n - b_g - \eta_g)^\wedge \Delta t) \\ v_{n+1} &= v_n + g\Delta t + R_n(\tilde{a}_n - b_a - \eta_a) \\ p_{n+1} &= p_n + v_n\Delta t + \frac{1}{2}g\Delta t^2 + R_n(\tilde{a}_n - b_a - \eta_a)\Delta t^2 \end{aligned} \quad (1)$$

where R_n , v_n , and p_n are orientation, velocity and position of the sensor with respect to the world, respectively, and Δt is the sampling time of the IMU. The angular velocity and acceleration measurements $\tilde{\omega}_n, \tilde{a}_n$ from the gyroscope and accelerator are contaminated with additive Gaussian noise η_g, η_a and random walk bias terms b_g, b_a . In the above model, these noise terms have been subtracted from the sensor measurements to yield the ideal angular velocity and accelerations. Furthermore, the $\text{Exp}(\cdot)$ function in the above equation is the SO3 exponential map that converts the skew symmetric members of the lie algebra $\mathfrak{so3}$ to their corresponding SO3 matrix.

As it can be seen in the above equation, the new orientation R_n , velocity v_n , and position p_n are functions of initial values whose change forces the recalculation of the whole integration. To address this issue for Visual Inertial Odometry (VIO) algorithms, [10] proposes an inertial constraint independent from the initial states and only functions of the sensor measurements. Known as preintegrated IMU factors, this constraints can compress the consecutive IMU samples into a single constraint (vector). For IMU measurements between time i and

j this may be achieved using the following definition [10]:

$$\begin{aligned} \Delta R_{ij} &\triangleq R_i^\top R_j = \prod_{k=i}^{j-1} \text{Exp}((\tilde{\omega}_k - b_k^g - \eta_k^g) \Delta t) \\ \Delta v_{ij} &\triangleq R_i^\top (v_j - v_i - g\Delta t_{ij}) \\ &= \sum_{k=i}^{j-1} \Delta R_{ik} (\tilde{a}_k - b_k^a - \eta_k^a) \Delta t \\ \Delta p_{ij} &\triangleq R_i^\top \left(p_j - p_i - v_i \Delta t_{ij} - \frac{1}{2} \sum_{k=i}^{j-1} g \Delta t_k^2 \right) \\ &= \sum_{k=i}^{j-1} \left[\Delta v_{ik} \Delta t + \frac{1}{2} \Delta R_{ik} (\tilde{a}_k - b_k^a - \eta_k^a) \Delta t^2 \right] \end{aligned} \quad (2)$$

where the initial states terms have all been moved to the left hand side of the equation.

In this paper, we exploit this idea to generate compressed and efficient input feature vectors from the raw IMU data that encode the motion between consecutive points encapsulating a number of IMU measurements. Calling them PreIntegrated (PI) features, we calculate them using the right-hand side of the above equations, given an arbitrary division of the raw data into batches of N IMU samples. Thus, the greater the N , the more compressed the eventual feature vector. Furthermore, each PI feature is a 9D vector comprised of concatenating the ΔR_{ij} , Δv_{ij} , and Δp_{ij} factors as follows:

$$PI_k = [\log(\Delta R_{k,k+ID})^\vee, v_{k,k+ID}, p_{k,k+ID}]^T \quad (3)$$

where $\log(\cdot)$ is the SO3 logarithmic map, and ID indicates the integration depth and is the number of samples compressed into the vector.

It is important to note that since we aim to use these features as inputs to deep learning models, we may eliminate the noise terms from the above equations and rely on the model to compensate for their impact. Nevertheless, similar to the approach proposed by [11], one may use the noise characteristics of the IMU to generate random values for these terms, which in turn, would serve as a data augmentation scheme and makes the model more robust against these noise effects.

B. Network Architecture

As proposed by the authors of the IO-Net [12], this paper formulates the pedestrian inertial odometry as a sequence learning problem. This approach mitigates the growing error issue of classic odometry methods which is due to the trapped initial velocity and orientation errors in the propagation formulation of Equ1. Specifically, the raw IMU data are broken into separate windows of 200 samples (2 seconds) and each window is individually processed by the model to yield the odometry output $(\Delta L, \Delta \Phi)$ presented in polar coordinates.

Each odometry output updates the subject’s position based on the following formula:

$$\begin{cases} \Phi_{n+1} &= \Phi_{n-1} + \Delta\Phi \\ X_n &= X_{n-1} + \Delta L \cos(\Phi_n) \\ Y_n &= Y_{n-1} + \Delta L \sin(\Phi_n) \end{cases} \quad (4)$$

Based on the above equation, the old heading Φ_n is updated using the $\Delta\Phi$ odometry output. The updated Φ_{n+1} is then used alongside the odometry output ΔL to update the position $P_n = [X_n, Y_n]^T$.

Similar to IO-Net, the measurement windows are generated with a stride of 10 to increase the inference frequency. This way, the position measurements may be updated every 100ms instead of 2 seconds.

The IO-Net’s architecture has been illustrated in Figure 1.a. The model is comprised of two bi-directional LSTM layers with 128 and 258 numbers of units for the first and the second layer. The last hidden state of the second layer’s LSTM is fed into two linear layers to produce the polar odometry predictions. Furthermore, the input of the first layer is fed by a fully connected 2-layer MLP that maps the 6D IMU measurements to a 128 channel input feature. Therefore, the base model takes a 200×6 dimension IMU sequence and produces a single 2D polar output vector.

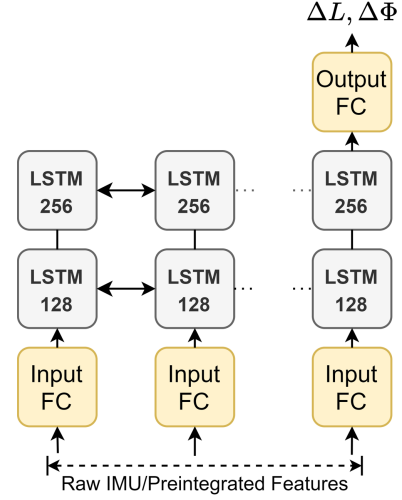
For investigating the preintegrated features, the IMU samples are replaced with the 9D preintegrated vectors calculated by the custom layer. In this case, the input to the model would be a sequence of features with a $200/ID \times 9$ dimension. In this formula, ID indicates the integration depth, which is the number of raw samples used for calculating each preintegrated feature. This temporally compressed input feature enables one to use a shallow CNN to process the sequence. Figure 1.b illustrates such a model. Designed for our embedded implementation, this model is comprised of two convolution layers flowed by a 2-layer fully connected MLP with ELU activation and 32 neurons in the first layer. Compared to the LSTM baseline with 1.3M parameters, this CNN model is considerably smaller and has only 11K parameters, which is suitable for the embedded implementation on a microcontroller.

C. Loss Function and Training Procedure

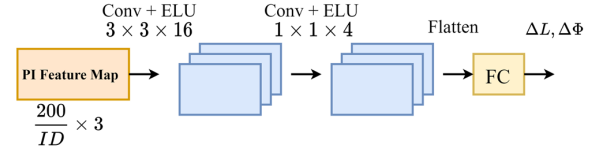
The loss function for training all the models in this paper is of the following form:

$$L = \sum_{i=1}^N \|\Delta L_i - \Delta \hat{L}_i\|_2^2 + \beta \|\Delta \Phi_i - \Delta \hat{\Phi}_i\|_2^2 \quad (5)$$

where N is the number of training sequences, $\Delta L_i, \Delta P h i_i$ are the network’s outputs, and $\Delta \hat{L}_i, \Delta \hat{\Phi}_i$ are the ground-truth labels. Furthermore, the β hyperparameter in the above equation provides a balance between the orientation and translation components of the loss. This paper sets this parameter based on the average norm of the orientation and translation losses on a randomly initialized model such that the two terms would contribute equally in the backpropagation.



(a) Baseline IO-Net



(b) Small CNN Model

Figure 1: (a) The IO-Net base model architecture for investigating the effectiveness of preintegrated features. (b) The proposed CNN model for the embedded implementation of pedestrian odometry.

$\Delta \hat{\Phi}_i$ heading label is the projection of the orientation difference between the first and the last sample in the window which is calculated as follows:

$$\Delta \hat{\Phi}_i = \log(R_i^T R_{i+199})_z^v \quad (6)$$

where $\log(\cdot)$ function in the above equation is the $SO3$ logarithmic map and R_i represents the ground-truth label for the i^{th} sample in the window. Furthermore, $\Delta \hat{L}_i$ is calculated as the Euclidean distance between the x-y projections of the first and the last position vector in the window:

$$\Delta \hat{L}_i = \sqrt{(X_i - X_{i+199})^2 + (Y_i - Y_{i+199})^2} \quad (7)$$

Moreover, in order to avoid overfitting, this paper adopts dropout layers with probability 0.2 after each LSTM units, and furthermore, between the fully connected layers.

III. RESULTS

A. Dataset and Setup

This paper utilizes the Oxford Inertial Odometry Dataset (OxIOD) [12] to train the baseline and proposed models. The majority of data in this dataset have been collected using the IMU sensor of an iPhone 7 plus smartphone and a Vicon motion capture system as ground truth.

The ground-truth provides accurate measurements ($0.5mm$) of the subject performing various modes of motion, such as halting, slow walking, and running while the phone is placed on various positions such as in the pockets, handbag, handheld, and on a trolley. The total distance and recording time of this dataset are 42.5Km and 14.75 hours. In this paper, this dataset has been chosen following the baseline IO-Net with identical train and test set splits to provide a fair comparison.

The models and the training pipelines have been developed using Pytorch [13] and PyTorchLightning [14]. Furthermore, Adam optimizer with an initial learning rate of $1e - 3$, and default moment parameters have been used to train the model. Furthermore, an exponential learning rate scheduler with $\alpha = 0.9$ has been used to reduce the learning rate with each epoch. The CNN embedded model has been implemented using Keras [15] as it was a requirement for porting the model on a microcontroller. All the codes for this paper are available at our GitHub repository ².

The embedded implementation of the CNN model is done using the X-Cube-AI framework [16], and the preintegration processing has been implemented using the highly optimized ARM CMSIS-DSP math library. While we could have quantized the Keras model for improving its performance, we used the floating-point version due to its generality and faster implementation. On the lowest level of the X-Cube-AI framework, a run-time utilizes the ARM CMSIS-NN/DSP libraries [17] to run the converted Keras networks efficiently. The user application may then load the run-time with the appropriate network for inference. Here, the implementation has been done using an ARM STM32F407ZET microcontroller with 198KBi of RAM and 512KBi of flash memory, and with a Cortex-M4 CPU running at 168Mhz.

B. Baseline With and Without Preintegration

The effectiveness of preintegrated features has been investigated through applying the IO-Net model once with the raw IMU data and then, with the preintegrated features. For each case, the training procedure has been performed for identical numbers of epochs and batch sizes, and the preintegration depth has been chosen to be 10. Furthermore, following the IO-Net paper, the window size has been chosen to be 200 samples (2 seconds) to provide a fair comparison. This paper only focuses on data domains where the IMU is attached to the body and not on the trolley. Throughout the experiments, it was observed that the distribution for the trolley domain is fundamentally different compared to the on-body domains since it does not reflect the underlying patterns of human walking.

Furthermore, the Root Mean Square Error (RMSE) metric has been adopted for comparing the results quantitatively. Instead of comparing the integrated paths, we opt to compare the odometry outputs since it provides a more direct comparison. In VIO literature, this procedure is an accepted norm for comparing the performance of odometry algorithms [18].

Table I presents the model’s performances on slow walking, running, phone in pocket, and phone in the handbag domains. The reported numbers are the average rate of change for the heading and stride predictions, $(\Delta L/\Delta T, \Delta\Phi/\Delta T)$. The first and the second columns present the baseline model’s performance with raw and preintegrated features as inputs, while the third column presents the small CNN model’s performance. As seen in the first and second columns, the mode’s performance in predicting both heading and stride improves by replacing the raw inputs with preintegrated features. This improvement may be attributed to the fact that the preintegration’s intrinsic motion propagation releases the network from the duty of directly inferring them from the raw data. Notably, the ΔL improvement in the running domain is more prominent because the distance and the speed of the user are larger compared to other domains. Thus, the inference of ΔL from raw data and in the case of running would be more difficult. Furthermore, the $\Delta\Phi$ ’s improvement due to preintegration in the Handbag domain is more significant because direct heading inference from raw data would be more difficult due to the bag’s swing motion.

Furthermore, Figure 2 illustrates the qualitative results. The rows in the grid present the domain performances, and each column corresponds to a model. Furthermore, Each figure is comprised of two sub-figures representing the heading and stride predictions. As shown in the first and second columns of the figure, the model’s performance using preintegrated features are qualitatively similar to the baseline. However, the running domain appears more challenging due to the larger displacements and the more chaotic motion pattern. This randomness and the reduced number of samples lead to increased prediction noise. Following the same lead as the baseline paper [12], this problem may be mitigated using a small digital low-pass filter after the model and before integrating the odometry predictions.

In addition to the accuracy improvement, the temporally compressed preintegrated features lead to significant inference and training acceleration. Based on our experiments, an integration depth of 10 leads to more than $10\times$ inference and $6\times$ training acceleration.

C. Preintegration vs Downsampling

Similar to downsampling, preintegration reduces the number of samples to be processed by the model. Nevertheless, preintegration compresses the raw samples instead of throwing them away.

²The repository will be initiated by the time of acceptance.

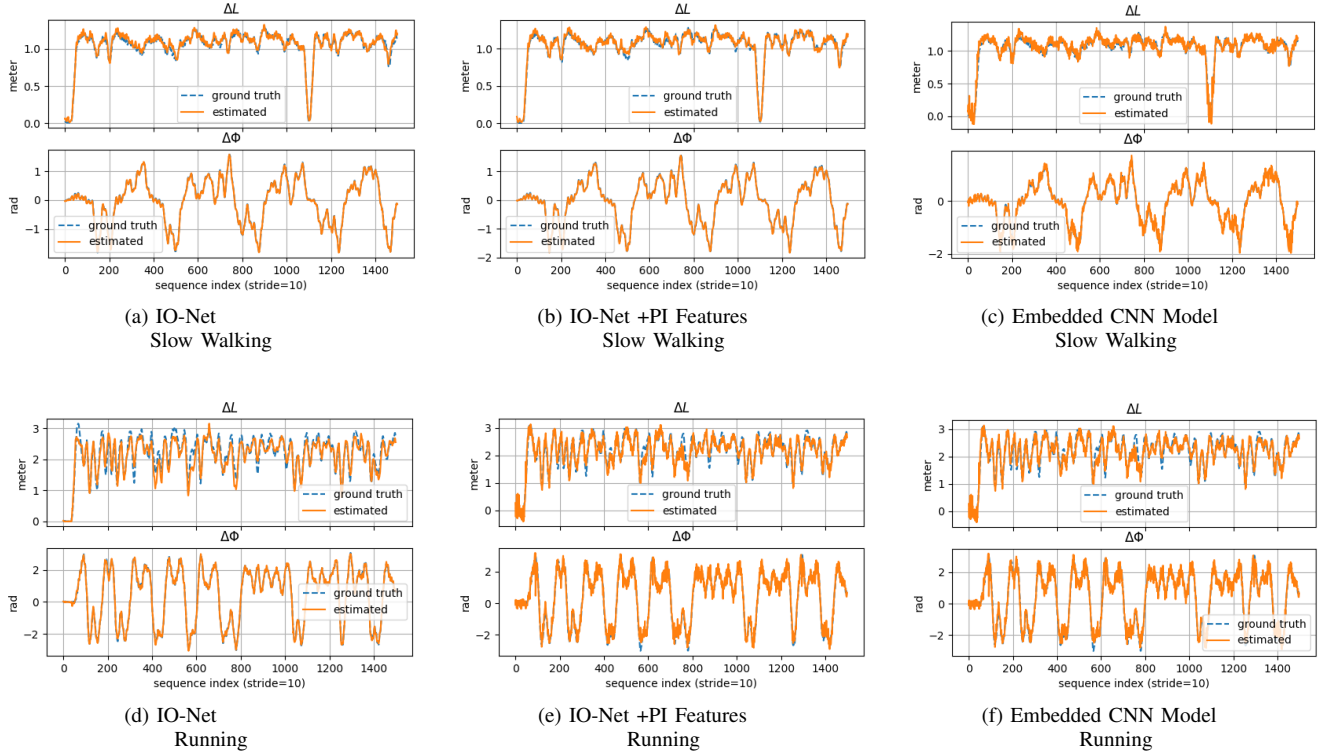


Figure 2: Qualitative comparison of the models with preintegrated inputs and the IO-Net baseline on two separate domains of slow walking and running.

Table I: RMS error of CNN and LSTM models with preintegrated features as inputs compared to the IO-Net baseline model with raw IMU input.

	Base Model ($\Delta L(m/S), \Delta \Phi(rad/S)$)	Model with Preintegrated Input ($\Delta L(m/S), \Delta \Phi(rad/S)$)	Embedded CNN Model ($\Delta L(m/S), \Delta \Phi(rad/S)$)
Slow Walking	(0.18, 0.013)	(0.017, 0.013)	(0.029, 0.013)
Running	(0.125, 0.255)	(0.1, 0.216)	(0.115, 0.26)
Pocket	(0.0141, 0.025)	(0.014, 0.025)	(0.021, 0.027)
Handbag	(0.041, 0.0261)	(0.032, 0.081)	(0.048, 0.081)

Table II: Preintegrated input features compared to downsampling.

Integration Depth / Downsampling Factor	Model RMSE with Downsampled Input ($\Delta L(m/S), \Delta \Phi(rad/S)$)	Model RMSE with Preintegrated Input ($\Delta L(m/S), \Delta \Phi(rad/S)$)
10	(0.043, 0.084)	(0.032, 0.081)
20	(0.053, 0.108)	(0.041, 0.085)
40	(0.068, 0.108)	(0.053, 0.085)
50	(0.075, 0.12)	(0.063, 0.085)

Table III: Resource consumption and performance on an *STM32F407ZET* microcontroller with 512KBi of Flash and 192KBi of RAM running at a clock frequency of 168MHz.

Process	RAM Usage (KBi)	ROM Usage (KBi)	Execution Time (ms)
Preintegration (per vector)	4 (Stack Size)	0 (No Parameters)	0.2
Model Inference	12.28	92.55	5

Table II illustrates the base model’s performance with downsampled inputs compared to that of preintegration. As it can be seen, as the downsampling factor increases, the accuracy drops. Nevertheless, preintegration consistently yields higher accuracy and a slower rate of performance drop for both ΔL and $\Delta\Phi$ components. Notably, the $\Delta\Phi$ component is least affected by the value of integration length/downsampling factor which may be explained by the IMU model in Eq. 1. Based on this model, estimation of the orientation is less demanding since it directly relates to the gyro measurement and is not affected by velocity and position initial states. However, traveled distance (ΔL) is affected by both gyroscope and accelerator measurements and is a function of initial orientation and velocity. Interestingly, in the case of preintegration, the performance drop of $\Delta\Phi$ is meager while there is a deterioration in downsampling. Nevertheless, the performance drop in downsampling and preintegration are roughly equal, while the absolute value of the error in preintegration is lower than downsampling. It is worth noting that this section’s experiment has also been performed on the other motion domains with similar results.

D. Performance on a Microcontroller

As indicated previously, the temporally compressed preintegrated features enable even shallower CNNs to cover a larger receptive field of the motion signal. As a result, one may drastically shrink the model’s dimension so it could be implemented on a microcontroller.

The quantitative results of this experiment have been shown in the third column of table I. Furthermore, the qualitative results have been illustrated in Figures 2.c and 2.f. As shown in the table, the model’s inference accuracy is on par with the baseline IO-Net. Similar to the analysis described previously, the $\Delta\Phi$ component of the predictions is least affected by the performed compression, and the ΔL component in the running domain has the largest error due to the fast motions. Based on the qualitative results, the CNN model’s predictions are relatively more jittery and noisy, which, as mentioned before, whose impact may be mitigated by a small digital low-pass filter.

Table III presents the implementational details of the CNN model on an STM microcontroller. As seen in the table, calculating each preintegration vector (compressed of 20 IMU samples in this experiment) takes about 0.2ms while each model inference requires only 5ms of computational time. Assuming a stride of 20 (running the inference after each 20 IMU measurements), each inference requires calculating one preintegrated feature and running one model inference, which in total takes 5.2ms. Since this computation is only required every 200 milliseconds, there will be plenty of CPU time left for other user-specific tasks. Furthermore, the model’s memory consumption is reasonably low requiring only 92.55/512KBi of flash and 12.28/192KBi of RAM which leaves plenty of room for other user-specific data and code. Furthermore, the successful processing of the preintegration vectors in the

microcontroller required increasing the stack to 4KBi which is reported here as the approximate required RAM.

IV. CONCLUSIONS AND FUTURE WORKS

This paper proposed a computationally efficient motion representation for deep inertial odometry to address the computational efficiency challenges of deep ego-motion estimation and to unleash their powers in the embedded applications. The effectiveness of the proposed method was then demonstrated for the task of pedestrian inertial odometry, and its efficiency was shown through an embedded implementation on a microcontroller with restricted resources. Prominent directions for future research are applying preintegration for other applications such as human activity recognition and visual-inertial odometry.

REFERENCES

- [1] T. Sandy *et al.*, “ConFusion: Sensor Fusion for Complex Robotic Systems using Nonlinear Optimization,” *IEEE Robotics and Automation Letters*, vol. PP, no. c, 2019. [Online]. Available: <http://arxiv.org/abs/1806.07115>
- [2] G. Huang, “Visual-inertial navigation: A concise review,” *Proceedings - IEEE International Conference on Robotics and Automation*, vol. 2019-May, 2019.
- [3] B. Wagstaff, V. Peretroukhin, and J. Kelly, “Robust Data-Driven Zero-Velocity Detection for Foot-Mounted Inertial Navigation,” *IEEE Sensors Journal*, vol. 20, no. 2, 2020.
- [4] M. Brossard, A. Barrau, and S. Bonnabel, “RINS-W: Robust Inertial Navigation System on Wheels,” *IEEE International Conference on Intelligent Robots and Systems*, 2019.
- [5] P. Kasnesis, C. Z. Patrikakis, and I. S. Venieris, “PerceptionNet: A deep convolutional neural network for late sensor fusion,” *Advances in Intelligent Systems and Computing*, vol. 868, no. September, 2018.
- [6] C. Chen *et al.*, “IoNet: Learning to cure the curse of drift in inertial odometry,” *32nd AAAI Conference on Artificial Intelligence, AAAI 2018*, 2018.
- [7] —, “Deep neural network based inertial odometry using low-cost inertial measurement units,” *IEEE Transactions on Mobile Computing*, 2019.
- [8] Y. Almalioglu *et al.*, “SelfFVIO: Self-Supervised Deep Monocular Visual-Inertial Odometry and Depth Estimation,” 2019. [Online]. Available: <http://arxiv.org/abs/1911.09968>
- [9] M. R. U. Saputra *et al.*, “DeepTIO: A deep thermal-inertial odometry with visual hallucination,” *IEEE Robotics and Automation Letters*, vol. 5, no. 2, 2020.
- [10] C. Forster *et al.*, “On-Manifold Preintegration for Real-Time Visual-Inertial Odometry,” *IEEE Transactions on Robotics*, vol. 33, no. 1, 2017.
- [11] M. Abolfazli Esfahani *et al.*, “AbolDeepIO: A Novel Deep Inertial Odometry Network for Autonomous Vehicles,” *IEEE Transactions on Intelligent Transportation Systems*, vol. 21, no. 5, 2020.
- [12] C. Chen *et al.*, “Deep-Learning-Based Pedestrian Inertial Navigation: Methods, Data Set, and On-Device Inference,” *IEEE Internet of Things Journal*, vol. 7, no. 5, 2020.
- [13] A. Paszke *et al.*, “Pytorch: An imperative style, high-performance deep learning library,” in *Advances in Neural Information Processing Systems* 32, 2019.
- [14] W. Falcon, “Pytorch lightning,” *GitHub*. Note: <https://github.com/PyTorchLightning/pytorch-lightning> Cited by, vol. 3, 2019.
- [15] F. Chollet *et al.*, “Keras,” <https://keras.io>, 2015.
- [16] “Getting started with X-CUBE-AI Expansion Package for Artificial Intelligence (AI) UM2526 User manual,” Tech. Rep., 2020.
- [17] ARM, “CMSIS DSP Software Library,” 2020. [Online]. Available: <http://www.keil.com/pack/doc/CMSIS/DSP/html/index.html>
- [18] M. Grupp, “evo: Python package for the evaluation of odometry and slam,” <https://github.com/MichaelGrupp/evo>, 2017.